

Cooling Enhancement of Electric Motors

Authors : Yasser G. Dessouky* and Barry W. Williams**

Dept. of Computing & Electrical Engineering

Heriot-Watt University

Riccarton, Edinburgh

EH14 4AS, U.K.

Fax : (+44)-0131-451-3327/3431

*** e-mail : ygd@cee.hw.ac.uk**

**** e-mail : bww@cee.hw.ac.uk**

Cooling Enhancement of Electric Motors

- Abstract

A new arrangement for the stator laminations of electric motors is presented which improves machine cooling. The arrangement is illustrated with static and dynamic comparisons between the new and the old arrangements of a 4-phase switched reluctance motor. The stator laminations, all of one design, are designed to provide either radially or axially oriented external cooling fins when stacked. The effective increase in heat dissipative surface area increases the full load output capacity, for a given copper winding temperature rise above ambient. The static test, with the rotor held stationary and a DC current fed to all phases, shows that for the same temperature increase of the copper parts above the ambient, the RMS phase current can be increased. When the motor is mechanically loaded, keeping the speed constant such that windage and friction losses are fixed, an improvement in the efficiency has been obtained for a given copper temperature rise.

List of symbols

A	:	surface area, m^2
h	:	heat transfer coefficient, $W/m^2\ ^\circ C$
I_{Link}	:	DC link current, A
I_{RMS}	:	RMS phase current, A
P_c	:	inverter, windage and friction and stray losses, W
P_{Cu}	:	copper losses, W
P_d	:	net power to be dissipated as heat, W
$P_{i/p}$:	input power to the machine, W
$P_{o/p}$:	net output power, W
R	:	steady state resistance per phase, Ω
R_θ	:	thermal resistance, $^\circ C/W$

T : electromechanical torque, Nm

$\Delta\theta$: temperature difference between the machine winding and ambient, °C.

1. Introduction

In electric machinery, one of the factors which limits the design aspect is heat flow and the cooling arrangements for the different parts of the machine [1]. A basic factor of all machine specifications is the total heat loss in the machine which is the main determinant of the temperature rise above ambient of the copper inside the machine. The reason for limiting the temperature rise is to avoid damage to the insulation. Heating of the machine is a function of its losses while cooling is a function of the facilities by which heat is dissipated to the outside media, such as air or oil. In steady-state, the final temperature is reached when the rates of production and dissipation of heat are equal. Improvement to the cooling of the machine will consequently result in decreasing the temperature rise or alternatively, in increasing the machine rating for the same thermal loading. At a basic level, the impact of one design parameter - the motor's external surface area A - can be related to temperature rise and power dissipation using the approximate single body

relation:

$$\text{-- 1) } \Delta\theta = R_{\theta} * P_d ,$$

where

$$R_{\theta} = 1/(h*A) ,$$

Thus, for the same temperature rise,

$$\text{-- 2) } P_d \propto (1/R_{\theta}) \propto A$$

This means the higher the surface area, A, the lower is the thermal resistance, the higher is the feasible power dissipation and consequently the higher the machine rating. This is applicable to any electric machine, and in this paper, is illustrated with reference to a low power 4-phase switched reluctance motor. In smaller machines cooling is dominated by mechanisms associated with equations 1 and 2. In larger machines other heat transfer mechanisms come into play.

2. Stator Lamination Design

The capacity of any body for heat dissipation is dependent on the contact surface between the body and the outside media and if this contact surface is enlarged, the thermal resistance is decreased. The objective is to provide a means of utilising the lamination external structure of the stator of an

electromagnetic machine to provide inherent cooling fins [2]. Previously, core stacks have used laminations to provide fins for cooling, but used different lamination punchings in achieving the effect [2].

The stator comprises a stack of laminations, each lamination providing cut-outs suitable for accommodating the rotor and an appropriate means of stator excitation. Each identical stator lamination is designed such that when stator laminations are appropriately stacked, cooling fins are formed on the exterior surface of the stator, which are radially or axially orientated with respect to the rotor [3]. Figure 1 shows a stator lamination design which is an embodiment of the concept. The stator poles are identical in geometry and located at 45° intervals around the interior cut-out. The back-iron thicknesses, t_a and t_b , are not equal.

Figure 2 shows the manner in which the stator lamination design of Figure 1 is utilised to form cooling fins.

Groups of one or more stator laminations are orientated at ninety degrees to each other whilst still maintaining the required interior stator pole configuration as shown in Figure 2a. When the stator laminations are interleaved in groups and stacked, the difference in back-iron thickness gives the shaded areas where each group of laminations protrudes from its neighbouring group by a distance given by the difference in the back-iron dimensions. When the stator lamination stack comprises such interleaved groups, the protruding areas $[(t_b - t_a) * 8 * \text{number of groups}]$ which form cooling fins provide extra surface area. In this case, the fins are radially oriented along the axial length of the stack as shown in figure 2b. In three-phase cylindrical machines, the stator lamination may be elliptical or eccentric in form with angular displacement of groups to one another of multiples of 60° or 120° electrical degrees, whilst still maintaining the desired stator-pole configuration. In all cases, only one lamination design is required. The lamination arrangement is such that the average back iron requirement is maintained. Figure 3 parts a and b show how the asymmetrical lamination orientation concept, using the same lamination shape, can be applied to the three phase motor. Figure 3c shows how longitudinal fins may be created [3].

3. Static test

The 4-phase SR motor used for tests, figure 4, is suitable for domestic white goods applications.

Motor details appear in table 1. A static comparison can be done between the new arrangement and the conventional arrangement, in which all laminations are assembled in one orientation. If the rotor is held stationary and a DC current (I_{dc}) is fed to all phases, in the steady state when the rates of production and dissipation of heat are equal, the net power, P_d , to be dissipated as heat are the copper losses, viz., $4 * I_{dc}^2 * R$. A set of readings for $\Delta\theta$ and P_d for different levels of P_d are measured. Figure 5a shows the

relationship between $\Delta\theta$ and P_d for each configuration. Figure 5b shows the relationship between $\Delta\theta$ and I_{dc} , from which it can be concluded that for $\Delta\theta$ equal to 80°C , (B class rating) according to the British Standard [4], the DC value and hence the RMS value of the phase current is improved by +6%.

4. Dynamic test

To show the thermal improvement aspect on load, the machine is loaded keeping the speed fixed at 2000 RPM (to fix windage, friction and stray losses). A PWM controller was used to maintain the current waveform as shown in figure 6, for which the RMS value is $(1/\sqrt{3})$ the maximum value of the current. The machine was run on load until the temperature stabilised throughout the machine. The following set of measurements were taken for different levels of I_{RMS} : Torque (T), DC link current (I_{Link}), the temperature rise of the coils above ambient ($\Delta\theta$) and, immediately after switching off, the winding resistance (R), enabling the following to be calculated:

$$P_{i/p} = V * I_{Link} \quad \text{-- 3)}$$

$$P_{o/p} = \omega * T \quad \text{-- 4)}$$

where V is the DC rail voltage (300 V), ω is the angular velocity (2000 RPM*2 /60, rad/s)

$$P_{cu} = 4 * I_{RMS}^2 * R \quad \text{-- 5)}$$

$$P_c = P_{i/p} - P_{o/p} - P_{cu} \quad \text{-- 6)}$$

Figure 7 shows the relationship between temperature rise $\Delta\theta$ and $P_{i/p}$, $P_{o/p}$, P_{cu} , P_c and efficiency, for both lamination orientations. The power flow diagram at $\Delta\theta = 80^\circ\text{C}$ for both configurations is shown in figure 8. It can be seen that the efficiency of this machine which is indirectly a function of temperature is improved from 34.2% to 35.1% (a 2.6% increase) under the operating conditions investigated. The output power is increased from 34.9W to 36.9W (5.7% increase). It should be noted that, in contrast to the situation during the static test, there is an extra source of cooling due to the rotor motion and extra losses, viz., the eddy and friction losses, which dissipate heat as well. In this machine, these sources of heating are not insignificant and therefore the improvement is not as high as for the static test.

The dc link power was measured rather than phase powers, because of the difficulties associated with measuring power (inparticular voltage) with sufficient bandwidth (the PWM frequency being 40 kHz). But the results remain valid relative to the conventional and new lamination arrangement, since inverter efficiency will be virtually the same in each case because the currents are very similar. Notwithstanding

this, it can be said that the overall drive efficiency (inverter + motor) was increased. This efficiency improvement is reflected by the machines stator core surface area increasing five fold , from 0.024m^2 to 0.122m^2 . The total machine surface area is increased from 0.05m^2 to 0.148m^2 (196% increase) when the area of the motor end caps is included. Both static and dynamic test were performed with the motor shaft horizontal and the motor frame 2" above a non-reflecting surface in a static environment. The motor is totally enclosed.

5. Discussion

The cooling arrangement may be implemented using one stator lamination design. Existing manufacturing techniques can be adapted to produce the laminations. The provision of adequate exterior surface area is most beneficial in applications where the machine is totally enclosed and hence through air ventilation is ruled out. An advantage is also gained in non-totally enclosed drives that use fan forced air cooling and where the machine is required to spend significant periods of time at low speeds. During low speed operation, the cooling fins compensate for the reduced air flow from the fan. In some machines, the external casing surrounding the stator core, features cooling fins. The interface between core and case adds an extra thermally resistive component to the cooling circuit of the convention motor. The presented arrangement avoids this by providing a direct interface between stator core and ambient surroundings. When the low permeability casing can be avoided, the back-iron of the stator constructed according to this paper can be greater for a given overall size, if an identical fin geometry is used in both cases. The increased space can alternatively be used to increase the outside diameter of the rotor whilst still maintaining the required air-gap length and back-iron. This increases the D^2L product of the machine, thereby improving output power. Conversely, the outside diameter of the machine using fin geometries stamped on the outside edge can be reduced and give the same back-iron area with the same power output but from a machine with a smaller volume. The exterior surface of the stator may be coated so as to inhibit iron oxidation and improve surface emissivity. Only one arrangement of the laminations has been presented, with lamination stacked in 4:3 groups. The actual depth and width of formed fin is highly dependent on the motor size. With longitudinal fins as in figure 3c the formed fins contribute little to the average back iron thickness. But such an arrangement is obviously better with fan cooling.

6. Conclusion

A novel stator cooling arrangement has been presented. A static and dynamic comparison between the old and the new arrangements has demonstrated that a useful improvement in performance can be achieved. The rating of the 200W 4-phase SR machine has been increased by 5.7% for a given volume and copper temperature rise. This arrangement can be adopted for alternating and direct current machines in both rotary and linear configurations.

7. Reference

1. Say, M.G.: 'Electrical engineering design manual' (Chapman and Hall Ltd., 1962) 3rd edn.
2. Patent 549356, ' Induction regulator', Laurence Scott, 1965.
3. Patent Application 9613513.2, ' Provision of cooling fins on the stator of Electro magnetic machines using lamination structures'.
4. British Standard 4999: 'General requirements for rotating electrical machines', part 101, specification for rating and performance, 1987.

Table 1. Motor details

Pole arc/pole ratio of stator = 0.45	Pole arc/pole ratio of rotor = 0.5
Outside frame dimensions (m ²) = 0.144×0.125	Bore diameter (m) = 65*10 ⁻³
Rotor inner diameter (m) = 42.5*10 ⁻³	Shaft diameter (m) = 15*10 ⁻³
Stack length (m) = 47.45*10 ⁻³	Back iron width (m) = 7*10 ⁻³
Air gap length (m) = 0.25*10 ⁻³	Lamination thickness (m) = 0.65*10 ⁻³
New arrangement = 11 groups*3 laminations + 10 groups*4 laminations	Phase resistance(Ω) = 9.6
Inductance ratio(L _{min} /L _{max}) = 0.3334	No. of turns per phase = 710
Total machine surface area(m ²) = 0.148	Total machine volume (m ³) = 1.96*10 ⁻³

List of captions

Figure 1 : A stator lamination design

Figure 2 : Stator lamination orientation to form cooling fins

Figure 3 : Lamination for (a), (b) asymmetrical lamination orientation concept and (c) for longitudinal fins
for a 3-phase machine

Figure 4 : The 4-phase SR motor used for tests

Figure 5 : The relationship of developed power P_d and phase current I_{dc} versus temperature rise, $\Delta\theta$

Figure 6 : The waveform of the four phase currents

Figure 7 : The relationship of (a) input power $P_{i/p}$, output power $P_{o/p}$, copper losses P_{cu} , maintained
constant losses P_c and (b) efficiency $\eta\%$ versus temperature rise, $\Delta\theta$

Figure 8 : The power flow diagram at $\Delta\theta = 80^\circ \text{C}$.

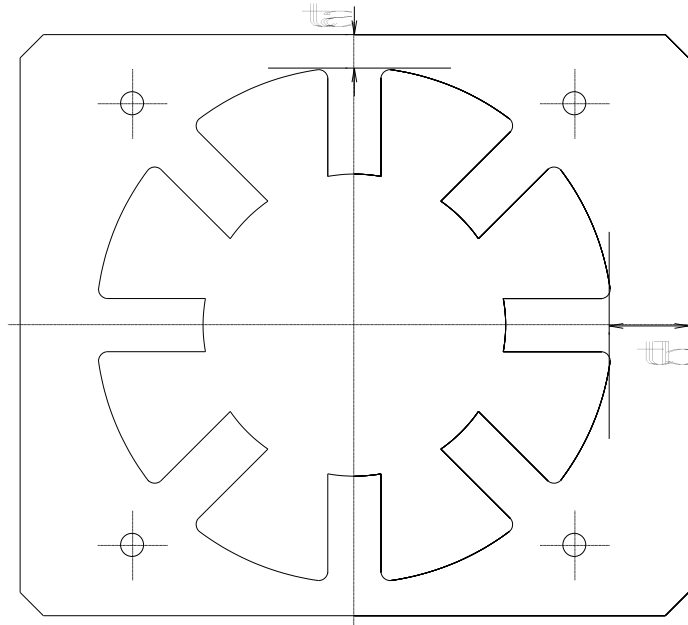


Figure 1. Astor laminations design

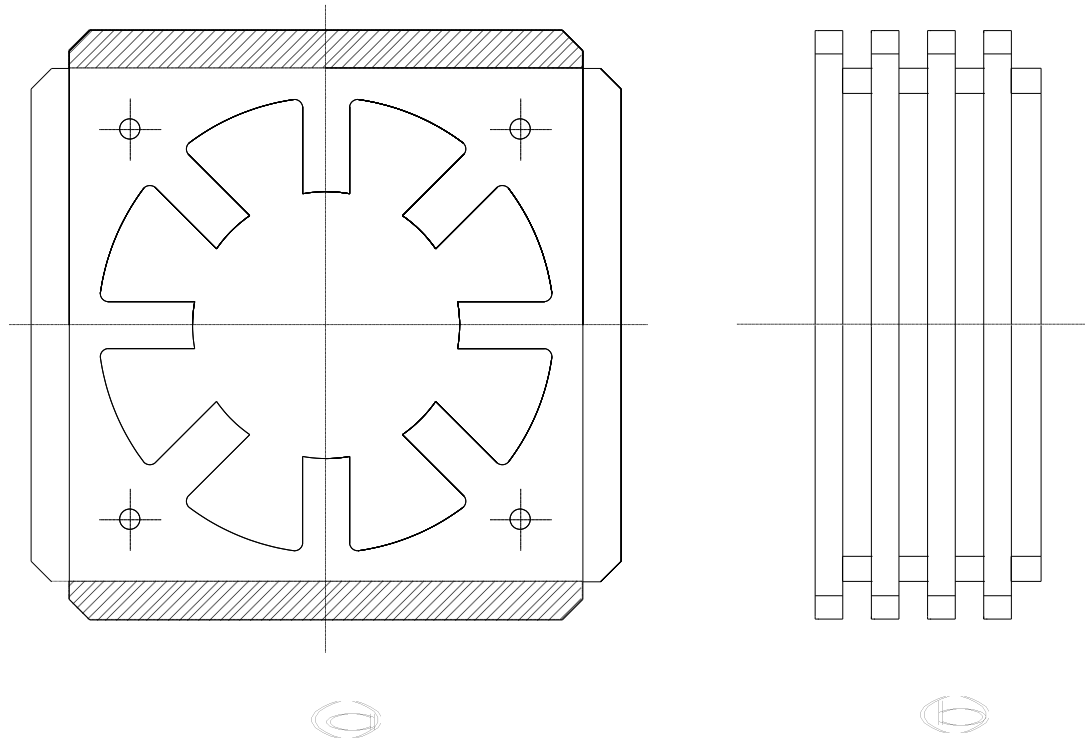
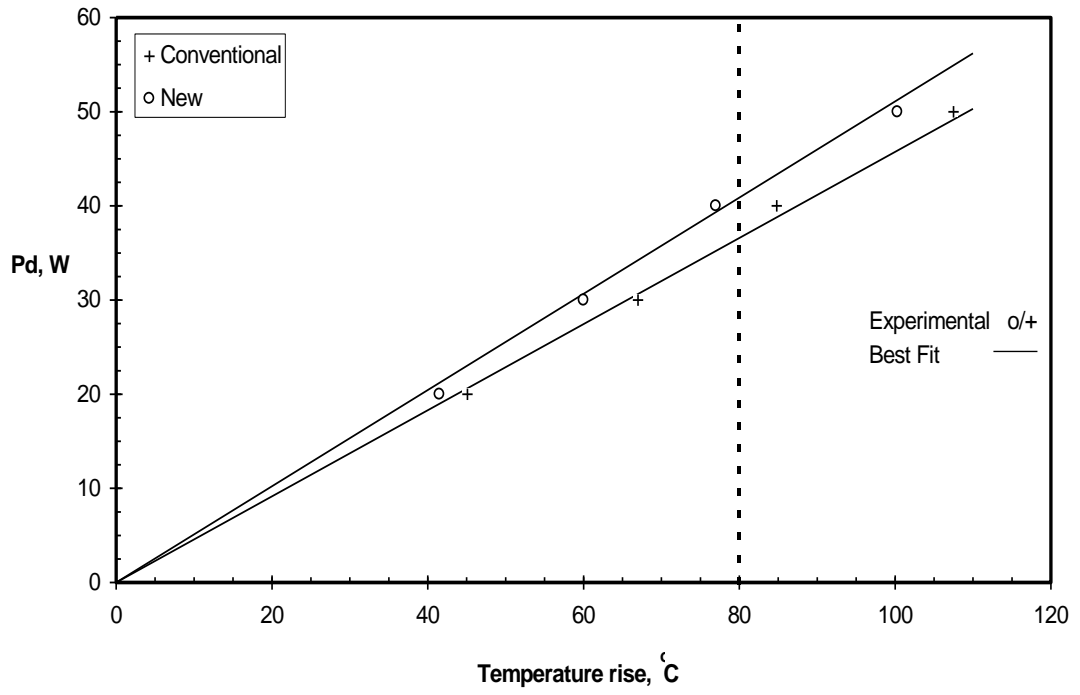
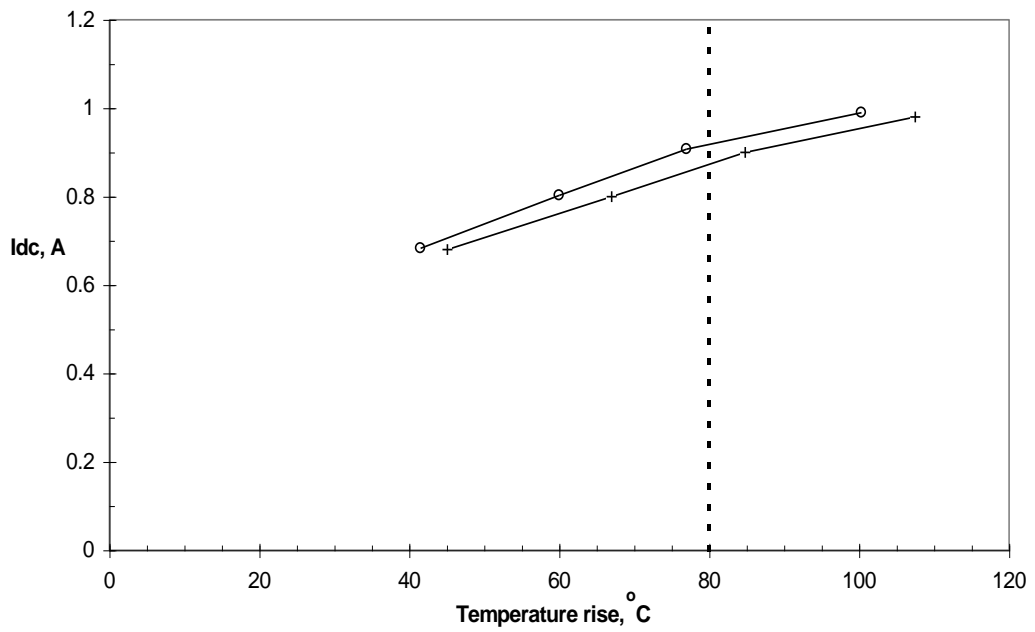


Figure 2. Lamination orientation to laminations

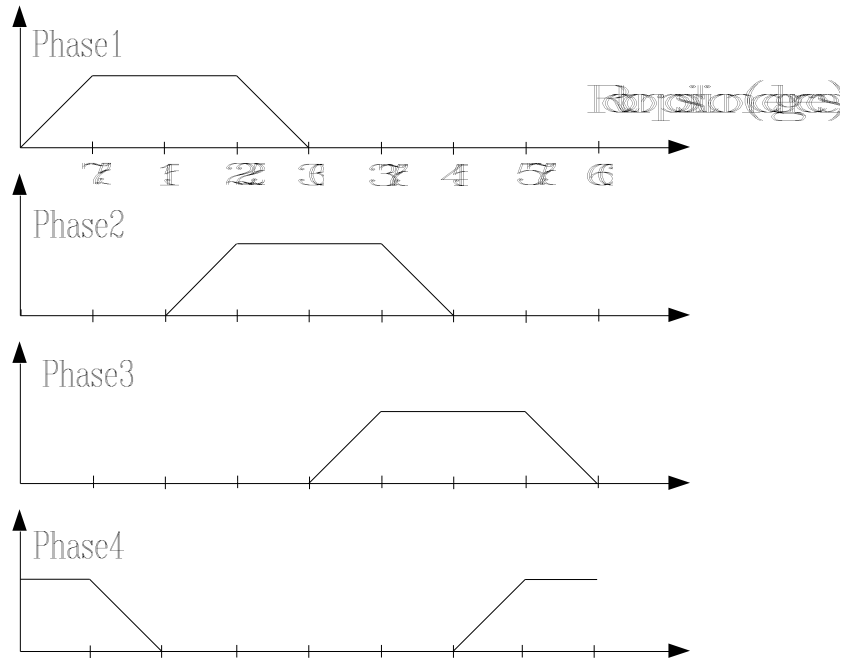


(a)



(b)

Figure 5 : The relationship of developed power P_d and phase current I_{dc} versus temperature rise $\Delta\theta$



Phase1 Phase2 Phase3 Phase4

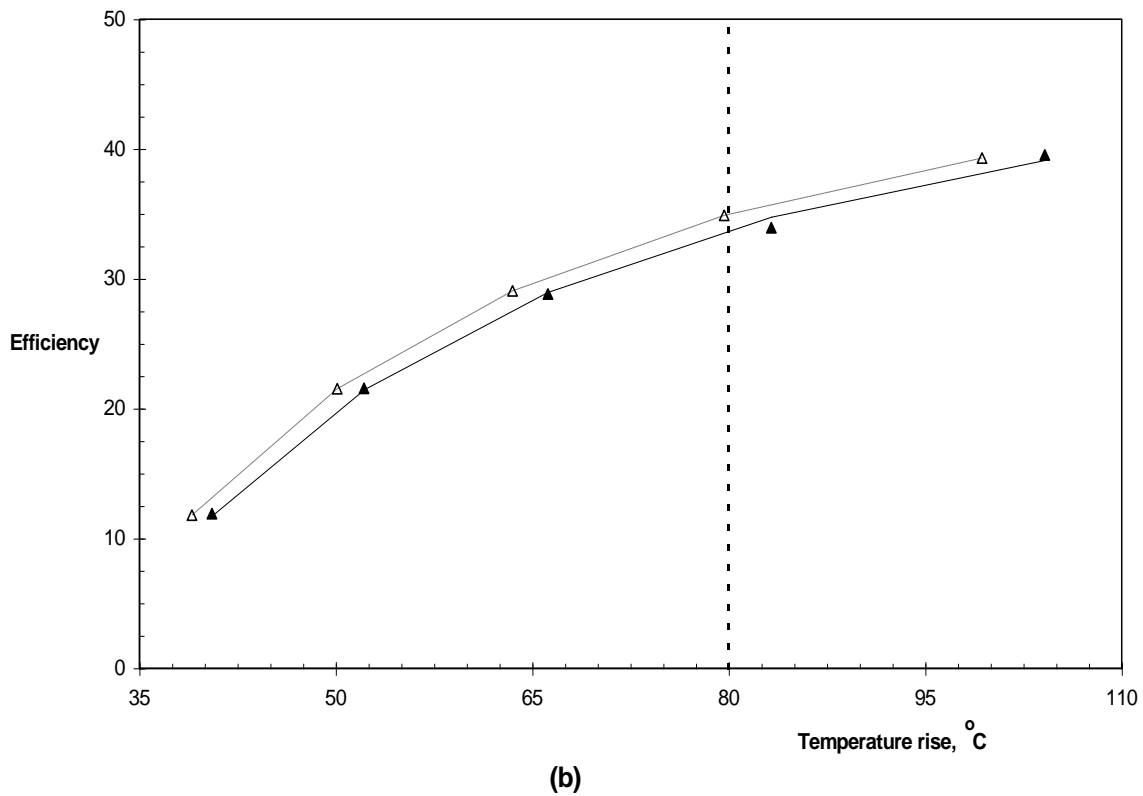
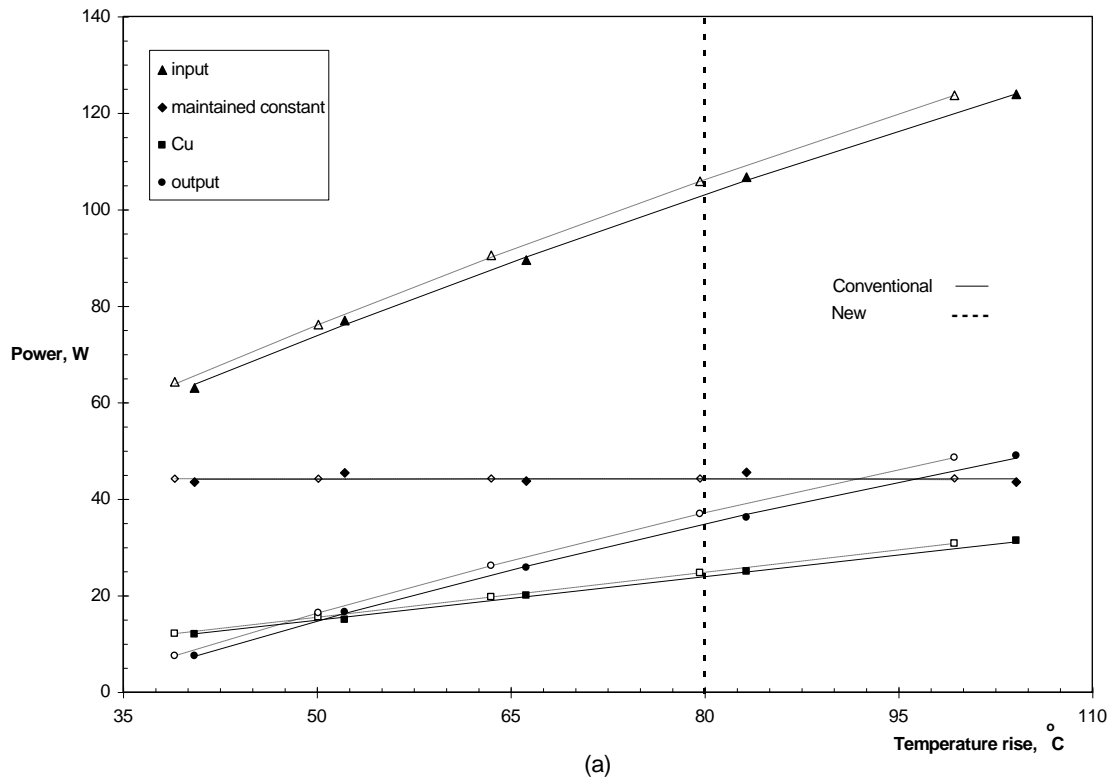
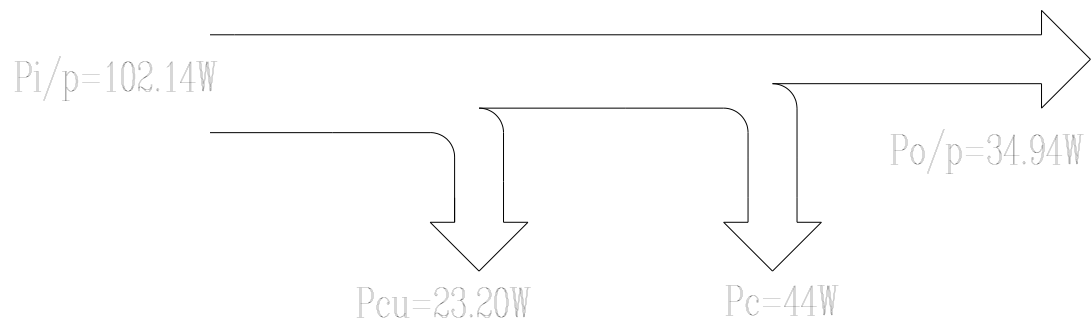
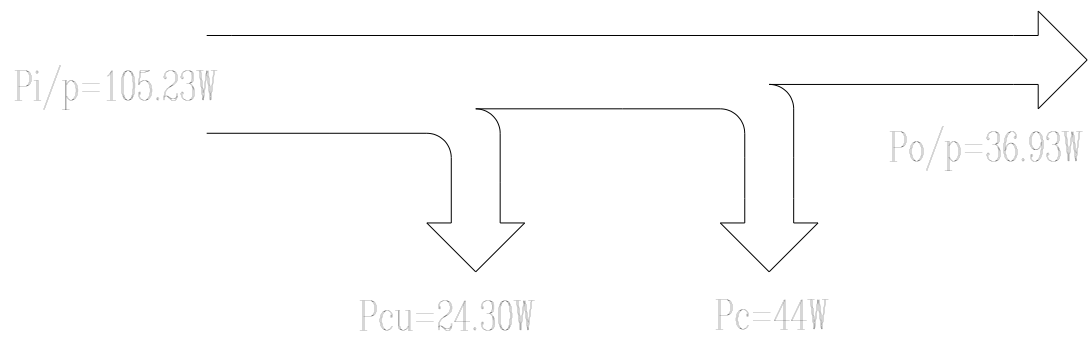


Figure 7 : The relation of input power P_i/p , output power P_o/p , copper losses P_{cu} , maintained constant losses P_c and efficiency $\eta\%$ versus temperature rise, $\Delta\theta$



(a) Conventional



(b) New

Figure 8: The power flow diagram at

$$\Delta\Theta = 50^{\circ}\text{C}$$